ENERGY COMPACTION CAPABILITY OF DCT AND DHT WITH CT IMAGE CONSTRAINTS

Chiou-Ting Hsu[1] and Ja-Ling Wu[1,2]

[1]Communication and Multimedia Lab.,
Department of Computer Science and Information Engineering,
National Taiwan University, Taipei, Taiwan
[2]Department of Information Engineering,
National Chi-Nan University, Puli, Nantou, 545, Taiwan
E-mail: f0506010@csie.ntu.edu.tw

Abstract: Since computerized tomography (CT) images have general structures consisting of an approximately elliptical region containing almost all of the image energy and are bounded by a region in which the image intensity is essential zero, the property must be introduced into the source model for performing transform coding analysis.

For 3-D CT image data sets, in order to take advantage of the time-domain correlation between contiguous images, the difference between consecutive images is encoded instead of the original one.

In this paper, energy compaction capabilities of DCT and DHT using 2-D source model (for spatial dependence) and difference model (for time dependence) with boundary constraints, both separable and non-separable, are explored. Experiments are performed to verify that DHT is suitable to be used in transform coding for CT data.

1. INTRODUCTION

Transform coding involves linear transformation in which the statistically dependent signals will be mapped into a set of more independent coefficients, where the transformed coefficients are then quantized and compressed. The function of the transformation is to make the transformed coefficients more independent than the original signal so that the subsequent operations of quantization and entropy encoding can be done more efficiently.

A considerable amount of researches have shown that the discrete cosine transform (DCT) is the best way to encode digital image information. For a highly correlated image (correlation coefficient $\rho \geq 0.5$) with a 1st-order Markov model, DCT approaches the optimum performance of the KLT [9].

However, for CT image compression, which have a roughly elliptical region of non-zero intensity bounded by a region with zero intensity, DCT loses its advantages over DFT [1]. It implies that, for CT images, DFT may get more compression gain than DCT does. But DFT maps real signal into complex spectrum, even though the symmetries of DFT of a real signal can be explored to reduce both the storage and computation, a transform that can directly map real signal into real spectrum and still preserve most of the useful properties of DFT is preferred. One such transform, closely related to DFT, is the discrete Hartley transform (DHT) [6].

In [1], 1-D source model and 2-D non-separable source model have been discussed. It was shown that the energy compaction efficiency of DFT is better than that of the DCT.

For 3-D CT image data sets, the main differences between consecutive images are due to motion and changes in body anatomy. In order to take advantage of the correlation between contiguous images, the difference image between the current image and the previous one is generated and encoded.

As compared to full-frame transformation, block transform coding requires less computation and memory, i.e., it is more suitable for those applications with bandwidth and real-time constraints. However, the blocking defect is visible and is unacceptable for medical applications [11]. The full-frame discrete cosine transform [10] has been developed to remedy this artifacts. Thus, we use the full-frame transform coding instead of the block one. In order to reduce the computational load, the fast algorithms for DCT, DHT and DFT [2]-[4] must be exploited.

In what follows, the energy compaction of 1-D and 2-D transform coding will be reviewed. Next, in Sec. 3 and 4 both 1-D and 2-D source models and difference models with CT image constraints will be discussed and used to compare the energy compaction ability of DCT, DHT and DFT. In Sec. 5, the experiments for compressing real CT images will be used to verify the validity of our models.

2. ENERGY COMPACTION

2.1. 1-D Transformation

Let $x(n)$ be a vector of length N, and the transformed vector $y(k)$ is given by: $y(k) = \sum_{n=0}^{N-1} T(k,n)x(n)$.

For DCT, DFT and DHT, $T(k,n)$ are as follows:

$$DCT:\ T(k,n) = \sqrt{2}c(k)/\sqrt{N}\ \cos\left(\frac{\pi(2n+1)k}{2N}\right)$$

$$where\ c(k) = \begin{cases} 1/\sqrt{2}, & if\ k = 0 \\ 1, & otherwise \end{cases}$$

$$DFT: T(k,n) = 1/\sqrt{N}\ \exp\left(-j\frac{2\pi kn}{N}\right)$$

$$DHT: T(k,n) = 1/\sqrt{N}\ cas\left(\frac{2\pi kn}{N}\right)$$

0-7803-4137-6/97/$10.00©1977 IEEE

Then, the variance of $y(k)$ can be expressed as

$$\sigma_y^2(k) = \sum_{n=0}^{N-1}\sum_{n'=0}^{N-1} T(k,n)r(n,n')T^*(k,n'),$$

where $r(n,n')$ is the covariance between $x(n)$ and $x(n')$.

We shall model x by a 1st-order Markov process with correlation ρ; therefore, $r(n,n') = \rho^{|n-n'|}$

2.2. 2-D Transformation

Now, let $x(m,n)$ be a 2-D 1st-order Markov process, and both $x(m,n)$ and $y(k,l)$ are N N images, then

$$y(k,l) = \sum_{m=0}^{N-1}\sum_{n=0}^{N-1} T(k,l,m,n)x(m,n)$$

The variance of the transformed coefficients is

$$\sigma_y^2(m,n) = \sum_{m,n,m',n'} T(k,l,m,n)r(m,n,m',n')T^*(k,l,m',n')$$

where r is the covariance between $x(m,n)$ and $x(m',n')$.

If the covariance is separable, the same ρ is assumed for both vertical and horizontal directions. In this case, $r(m,n,m',n') = \rho^{|m-m'|+|n-n'|}$

For non-separable case, the covariance function is

$$r(m,n,m',n') = \rho^d, \text{ and } d = \sqrt{(m-m')^2 + (n-n')^2}$$

2.3. Energy Compaction

In most practical cases, the signal energy is unevenly distributed in the transformed domain. The DC coefficient and some low-frequency ($y(k)$, $k \le$ K) coefficients tend to concentrate most of the signal energy. Thus, many transform coefficients ($y(k)$, k>K) can be discarded without much loss of information. The more signal energy a transform can pack in the first K coefficients, the better choice it is. For the highly correlated 1st-order Markov model, DCT have been shown to be near optimal for decorrelating images.

For difference images, adjacent pixels are much less correlated than those in the original images. Even though, in hybrid coders recommended in H.261 and MPEG, the transform coding is applied in both intraframe and interframe modes, and DCT was shown to be near optimal even for the motion compensated frame difference images [5].

3. SOURCE MODEL FOR CT IMAGES

CT images, which are characterized by a roughly elliptical region containing almost all the image data of interested, have a quite different structure with the other images [1]. In the following, the source model with CT image constraints will be discussed.

3.1. 1-D model

Consider a vector $x(n)$ of length N, which is 1st-order Markov for M < n < N-1-M, and the first and the last M values are zero. Then, the covariance is

$$r(n,n') = \begin{cases} \rho^{|n-n'|}, & M < n,\ n' < N-1-M \\ 0, & \text{otherwise} \end{cases}$$

Using this covariance, the set of the variances $\sigma_y^2(k)$ for the transform coefficients could be obtained. In order to get a more apparent comparison, the set of variances are evaluated numerically.

Figure 1 shows the normalized variances of DCT, DHT and DHT for N=16 with M=1. For M=0, it is the same as the ordinary first-order Markov model, and DCT performs better. While for M=1, i.e. CT model, either DHT or DFT packs more signal energy than DCT, and DFT and DHT perform almost the same.

Now, consider the relationships among DCT, DHT and DFT. Let $x_2(n) = x(n) + x(2N-1-n)$ be a symmetrical extension of $x(n)$.

One can find that

$$DCT_N\{x(n)\} = W_{2N}^{k/2} \cdot DFT_{2N}\{x_2(n)\}$$

$$DHT_N\{x(n)\} = \frac{1+j}{2}y(k) + \frac{1-j}{2}y(N-k),$$

$$\text{where } y(k) = DFT_N\{x(n)\}.$$

Thus the DCT is seen to be a phase factor times the DFT of the double length symmetrical extension of $x(n)$, while the DHT is applied to periodic $x(n)$ with period N and its properties are similar to those of the DFT. Figure 2 shows the periodicity associated with DCT and DFT(or DHT).

For nature images, placement of $x(0)$ next to $x(N-1)$ will introduce discontinuity into the signal, and thus its high frequency energy will be spread into the transform domain, therefore the energy compaction capability will be decreased. For these signals, the DCT which is applied to the smoother extended signals can have a better energy compaction efficiency. However, for the CT images, let $x(n)$ be one line of the CT images, Fig. 2 shows that the discontinuities of the DFT(or DHT) and the DCT periodic signals are almost the same. From Fig. 1, the DFT and DHT now have the better energy compaction capability than DCT does.

3.2. 2-D source model (separable covariance)

Now consider the 2-D separable case, the 1-D model is used both for the vertical and horizontal directions. Therefore, the covariance function is

$$r(m,n,m',n') = \begin{cases} 0, & (m,n) \text{ or } (m',n') \text{ ouside } D \\ \rho^{|m-m'|+|n-n'|}, & \text{otherwise} \end{cases}$$

where D is the elliptical region.

Fig. 3 shows the normalized variances $\sigma_y^2(k,l)$ of 2-D DCT, 2-D DHT and 2-D DFT for 16 16 image with elliptical region.

3.3. 2-D source model (non-separable covariance)

For the non-separable model,

$$r(m,n,m',n') = \begin{cases} 0, & (m,n) \text{ or } (m',n') \text{ outside } D \\ \rho^d, & \text{otherwise} \end{cases}$$

$d = \sqrt{(m-m')+(n-n')}$ *and D is the elliptical region.*

The simulation result is similar as separable case.

Similarly to the 1-D case, the 2-D DCT is seen to be the phase factors time the 2N 2N 2-D DFT of the

periodic symmetric extension of $x(m,n)$, while the 2-D DHT is applied to periodic image $x(m,n)$ of N N and its properties are similar to those of the 2-D DFT.

From Fig. 3, either DHT or DFT gets better performance for compressing CT images, with boundary constraints.

4. DIFFERENCE MODEL FOR CT IMAGES

Now, since the difference image is generated based on the previous one, it is modeled by mixing of a original first-order Markov process and a white noise process. Similarly, the CT image constraints will be included in this model.

4.1. 1-D difference model

Consider a difference vector $x(n)$ of length N, which is mixed by a 1st-order Markov (with correlation ρ) and a white noise (with a flat power spectrum) for $M<n<N-1-M$, and the first and the last M values are zero. Then, the covariance of $x(n)$ and $x(n')$ is

$$r_{diff}(n,n') = \begin{cases} \rho_{diff} \cdot \rho^{|n-n'|} + (1-\rho_{diff}) \cdot \delta(n-n'), \\ \qquad if\ M < n,n' < N-1-M, \\ 0, \qquad otherwise \end{cases}$$

where ρ_{diff} *is the correlation of consecutive frames.*

4.2. 2-D difference model (separable covariance)

Now consider the 2-D separable model, the 1-D model (27) is used both for the vertical and horizontal directions. Therefore, the covariance function is

$$r(m,n,m',n') = \begin{cases} 0, \quad (m,n)\ or\ (m',n')\ ouside\ D \\ \rho_{diff} \cdot \rho^{|i-i'|+|j-j'|} + \\ (1-\rho_{diff}) \cdot \delta(m-m') \cdot \delta(n-n'), otherwise \end{cases}$$

where D is the elliptical region

and ρ_{diff} *is the correlation of consecutive images.*

Fig. 4 shows the normalized variances $\sigma_y^2(k,l)$ for both 2-D DCT, 2-D DHT and 2-D DFT, for 16 16 images with $\rho_{diff} = 0.5$.

4.3. 2-D difference model(non-separable covariance)

For the non-separable case,

$$r(m,n,m',n') = \begin{cases} 0, \quad (m,n)\ or\ (m',n')\ outside\ D \\ \rho_{diff} \cdot \rho^{d} + \\ (1-\rho_{diff}) \cdot \delta(m-m') \cdot \delta(n-n'), otherwise \end{cases}$$

where $d = \sqrt{(m-m')+(n-n')}$, *D is the elliptical regio*

and ρ_{diff} *is the correlation of consecutive images.*

Figure 5 shows the normalized variances $\sigma_y^2(k,l)$ for both 2-D DCT, 2-D DHT and 2-D DFT, for 16 16 images with $\rho_{diff} = 0.5$.

5. EXPERIMENTAL VERIFICATION

Three CT images (CT1-CT3) and a non-CT image (Fruit) have been used to verify our source models, and two difference images are applied to the difference model. The three CT image are picked out of 64 CT images, and all the test images are of size 256 256, 8 bits/pel.

Table 2 and 3 show the energy compaction efficiency and the PSNR (peak signal-to-noise ratio) of the coefficient-discarded image and the original image, respectively. For CT images, DHT can obtain better compression performance than DCT either in original image or difference image. While for the Fruit image, DCT always performs better than DHT.

Table 2. Energy compaction efficiency of three real CT images(CT1-CT3) and one non-CT image.

Energy compaction efficiency of the first k parts of transform coefficients						
k		100%	80%	60%	40%	20%
CT1	DCT	1	**.99962**	**.99792**	**.99453**	**.98570**
	DHT	1	.99960	.99786	.99432	.98540
CT2	DHT	1	**.99952**	**.99831**	**.99573**	**.98750**
	DCT	1	.99950	.99827	.99560	.98710
CT3	DHT	1	**.99938**	**.99795**	**.99461**	**.98590**
	DCT	1	.99936	.99790	.99446	.98540
Fruit	DHT	1	.99964	.99907	.99736	.99380
	DCT	1	**.99965**	**.99907**	**.99819**	**.99550**

Table 3. Energy compaction efficiency of difference CT images (D1 and D2).

Energy compaction efficiency of the first k parts of transform coefficients						
k		100%	80%	60%	40%	20%
D1	DHT	1	**.96966**	**.86844**	**.71263**	**.44445**
	DCT	1	.96816	.86519	.70735	.43594
D2	DHT	1	**.98822**	**.96080**	**.91286**	**.77067**
	DCT	1	.98782	.95948	.90999	.76431

6. CONCLUSIONS

For CT images, the energy compaction capability of DHT/DFT is actually better than that of DCT. 1-D source model and 2-D non-separable model have been discussed in [1]. In this paper, in addition to 1-D source model and 2-D non-separable model, 2-D separable model is also discussed to verify the result. Moreover, the time dependence among 3-D CT images is taken into account to reduce the data volume.

In [5], it is shown that the source image and the (motion-compensated) difference image have the same KLT in spite of having different statistical characteristics, and DCT is still the best fixed fast transform for both types of images. However, for difference CT images, DCT is not the best choice any more. We follow the model established in [5], it is shown that DHT/DFT is still better than DCT for difference CT images. Experiments of real transforms, DCT and DHT, are performed to verify the results.

So far our discussion focused only on the energy compaction capability, and we have shown that DHT is actually a better real transform than DCT from the energy point of view. Bit allocation and entropy

coding should be designed and combined into our 3-D CT model to construct a complete compression algorithm, and this will be in our future work.

Reference

[1] J. D. Villasenor, "Alternatives to the Discrete Cosine Transform for Irreversible Tomographic Image Compression," *IEEE Trans. Med. Imaging*, vol. 12, no. 4, pp. 803-811, 1993.

[2] H. V. Sorensen, D. L. Jones, C. S. Burrus, and M. T. Heideman, "On Computing the Discrete Hartley Transform," *IEEE Trans. ASSP*, vol. ASSP-33, no. 4, pp. 1231-1238, Oct. 1985.

[3] J. L. Wu and S. C. Pei, "The Vector Split-Radix Algorithm for 2-D DHT," *IEEE Trans. SP*, vol. 41, no. 2, Feb. 1993.

[4] M. A. Haque, "A 2-D fast Cosine Transform," *IEEE Trans. on ASSP*, vol. ASSP-33, no. 6, 1985.

[5] C. F. Chen and K. K. Pang, "The Optimal Transform of Motion-Compensated Frame Difference Images in a Hybrid Coder," *IEEE Trans. Circuits and Systems*, vol. 40, no. 6, June 1993.

[6] R. P. Millane, "Analytic Properties of the Hartley Transform and their Implications," *Proc. IEEE*, vol. 82, no. 3, March 1994.

[7] P. Yip and K. R. Rao, "Energy Packing Efficiency for the Generalized Discrete Transforms," *IEEE Trans. Comm.*, vol. COM-26, no. 8, Aug. 1978.

[8] N. S. Jayant and P. Noll, *Digital Coding of Waveforms - Principles and Applications to Speech and Video*, Englewood Cliffs, NJ: Prentice Hall, 1984.

[9] K. R. Rao and P. Yip, *Discrete Cosine Transform : Algorithms, Advantages and Applications*, Academic Press, 1990.

[10] K. K. Chan, S. L. Lou, and H. K. Huang, "Radiologic image compression using full-frame cosine transform with adaptive bit-allocation," *Comput. Med. Imag. Graph.*, vol. 13, pp. 153-159, 1989.

[11] S. Wong, L. Zaremba, D. Gooden, and H. K. Huang, "Radiologic Image Compression - A Review," *Proc. IEEE*, vol. 83, no. 2, pp. 194-219, 1995.

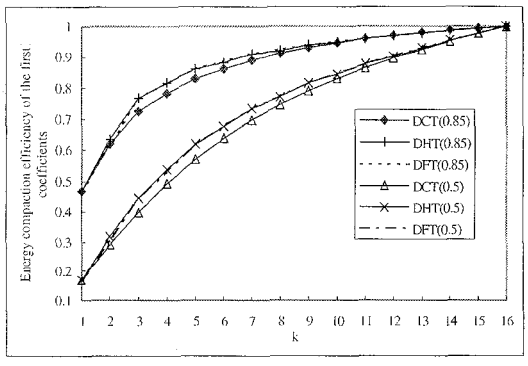

Figure 1. Energy compaction capability of DCT, DHT and DFT with different correlation, where M=1.

Figure 2. Periodicity of DCT and DFT (DHT), (a) one line of an CT image, (b) the periodic extension of DFT (DFT), (c) the periodic extension of DCT.

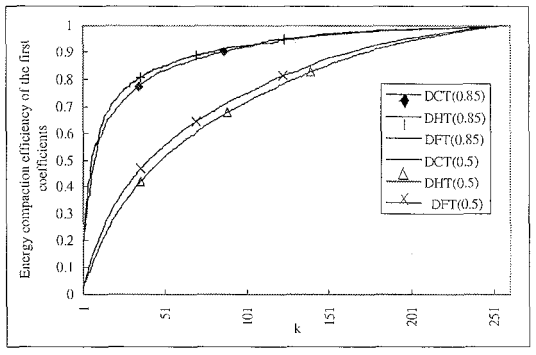

Figure 3. Energy compaction capability of 2-D DCT, 2-D DHT and 2-D DFT on separable model with correlation 0.85 and 0.5, where D is an elliptical region .

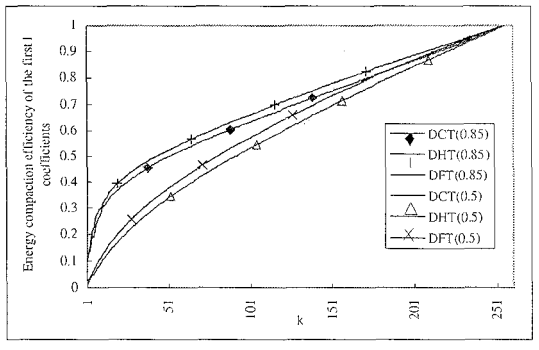

Figure 4. Energy compaction capability of 2-D difference image on separable model with $\rho_{diff} = 0.5$, where D is an elliptical region .

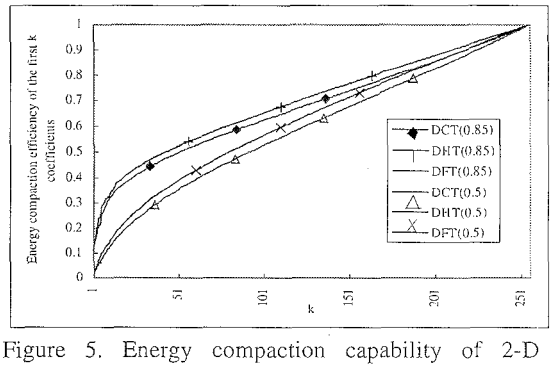

Figure 5. Energy compaction capability of 2-D difference image on non-separable model with $\rho_{diff} = 0.5$, where D is an elliptical region .